Global ionospheric response observed by COSMIC satellites during the January 2009 stratospheric sudden warming event

Xinan Yue,[1,2] William S. Schreiner,[1] Jiuhou Lei,[3] Christian Rocken,[1] Douglas C. Hunt,[1] Ying-Hwa Kuo,[1] and Weixing Wan[2]

Received 16 March 2010; revised 5 August 2010; accepted 11 August 2010; published 20 November 2010.

[1] This paper investigates the global ionospheric response during the January 2009 stratospheric sudden warming (SSW) event by using electron density profiles derived from GPS radio occultation measurements of the COSMIC satellites. The peak density (NmF2), peak height (hmF2), and ionospheric total electron content (ITEC) increase in the morning hours and decrease in the afternoon globally for 75% of the cases, in which electron density profiles during SSW and non-SSW days are available around the same location and local time bins. NmF2, hmF2, and ITEC during SSW days, on average, increase 19%, 12 km, and 17% in the morning and decrease 23%, 19 km, and 25% in the afternoon, respectively, in comparison with those during non-SSW days from global COSMIC observations. These results agree well with previous results from total electron content observations in low-latitude and equatorial regions. Interestingly, the unique COSMIC observations also revealed that during this SSW event the ionosphere responds globally, not only in the equatorial regions but also at the high and middle latitudes. The high-latitude ionosphere shows increased NmF2 and ITEC and decreased hmF2 in either the morning or afternoon sector. Thus, these results indicate that the ionospheric response in low-middle latitude and equatorial regions during SSW can be explained by either the modulated vertical drift resulting from the interaction between the planetary waves and tides through *E* region dynamo or the possible direct propagation of tides from the lower atmosphere, whereas the ionospheric variations at the middle and high latitude during the SSW might be attributed to the neutral background changes due to the direct propagation of tides from the lower atmosphere to the ionospheric F2 region. The competitive effects of different physical processes, such as the electric field, neutral wind, and composition, might cause the complex features of ionospheric variations during this SSW event.

Citation: Yue, X., W. S. Schreiner, J. Lei, C. Rocken, D. C. Hunt, Y.-H. Kuo, and W. Wan (2010), Global ionospheric response observed by COSMIC satellites during the January 2009 stratospheric sudden warming event, *J. Geophys. Res.*, *115*, A00G09, doi:10.1029/2010JA015466.

1. Introduction

[2] It is well known that many types of oscillations that originate terrestrially and in the lower atmosphere such as the acoustic-gravity waves, planetary waves, and tides can propagate to the upper atmosphere and result in fluctuation and disturbance of the ionospheric electron density through dynamic coupling processes [*Abdu et al.*, 2006; *Forbes and Leveroni*, 1992; *Fuller-Rowell et al.*, 2008; *Lăstovička et al.*, 2003; *Liu et al.*, 2010; *Rishbeth*, 2006; *Vineeth et al.*, 2007; *Wan et al.*, 1998; *Xiong et al.*, 2006; *Zhao et al.*, 2008]. These meteorological energy sources are thought to be the main contributors to the ionospheric day-to-day variability that cannot be explained by the solar forcing and geomagnetic activities [*Rishbeth and Mendillo*, 2001]. The stratospheric sudden warming (SSW) is one such typical phenomena that couples the stratosphere, middle and low altitude thermosphere (MLT), and upper atmosphere and ionosphere together. A SSW is an event where the polar vortex of westerly (eastward) winds in the Northern winter hemisphere abruptly slows down (minor SSW) or even reverses direction (major SSW), accompanied by a rise of stratospheric temperature by several tens of Kelvin [*Charlton and Polvani*, 2007]. Detailed description of SSW and its variations and physical mechanisms is beyond the subject of this paper and can be found in some reviews and outstanding papers [e.g., *Charlton and Polvani*, 2007; *Liu and Roble*, 2002].

[3] Many observations and modeling results have shown that the ionosphere can have dramatic changes during and

[1]COSMIC Program Office, University Corporation for Atmospheric Research, Boulder, Colorado, USA.
[2]Institute of Geology and Geophysics, Chinese Academy of Sciences, Beijing, China.
[3]Department of Aerospace Engineering Sciences, University of Colorado, Boulder, Colorado, USA.

0148-0227/10/2010JA015466

after a SSW event [e.g., *Chau et al.*, 2009; *Goncharenko and Zhang*, 2008; 2010a, 2010b; *Lăstovička and de la Morena*, 1987; *Liu et al.*, 2010; *Sridharan et al.*, 2009]. *Lăstovička and de la Morena* [1987] found that radio wave absorption in the lower ionosphere responds to a SSW event, depending on geographic location. A case study from *Sridharan et al.* [2009] showed that a SSW event can result in the reversal of the equatorial electrojet (EEJ) in the afternoon by enhancing the semidiurnal tidal amplitude. A SSW event usually occurs after the intensification of a planetary wave. *Vineeth et al.* [2007] analyzed the variations of daytime mesopause temperature and the EEJ strength over the dip equator during December 2005 to March 2006 period and indicated a possible strong dynamical coupling between the two regions through the intensification of planetary wave activity. *Chau et al.* [2009] reported that the vertical drift over Jicamarca had a semidiurnal variation with large amplitudes lasting for several days during the minor SSW event of 2008. *Goncharenko and Zhang* [2008] analyzed ion temperature at 100–300 km height observed by the Millstone Hill incoherent scatter radar that indicated alternating regions of warming in the lower thermosphere and cooling above 150 km altitude during the 2008 SSW event. Recently, using the National Center for Atmospheric Research (NCAR)-TIMEGCM model, *Liu et al.* [2010] performed a simulation to study the ionospheric variability due to the planetary waves and tides and obtained consistent variations of electric field and electron density observed during SSW event when quasi-stationary planetary waves become significant. It is now generally accepted that the intensified quasi-stationary planetary waves around the SSW event can interact with tides and lead to large changes of tides and thus result in the disturbance of the middle- and low-latitude ionosphere through the *E* region neutral wind dynamo [*Liu and Roble*, 2002; *Liu et al.*, 2010; *Sridharan et al.*, 2009].

[4] A major SSW event occurred during January 2009, when the solar activity was extremely low [*Manney et al.*, 2009; *Taylor and Randel*, 2009]. It provides a good opportunity to study the variability of the ionosphere resulting from the changes in the lower atmosphere. *Goncharenko et al.* [2010a, 2010b] investigated the low-latitude total electron content (TEC) variations during and after this major 2009 SSW event. They found that during the SSW period the TEC data in low-latitude and equatorial areas increase in the morning and decrease in the afternoon relative to the non-SSW period. The vertical drift observations in Jicamarca also showed strong variability during this SSW event [*Fejer et al.*, 2010]. This paper investigates the global ionospheric response during the 2009 SSW event using both lower atmospheric and ionospheric global positioning system (GPS) radio occultation (RO) observations from the Constellation Observing System for Meteorology, Ionosphere, and Climate (COSMIC), a joint U.S./Taiwan mission. COSMIC RO events provide both an ionospheric electron density profile (EDP) between the lower boundary of the ionosphere and the satellite altitude, and a neutral temperature profile between the Earth surface and ~60 km simultaneously in a similar geographic region. These collocated profiles allow us to study the connection between the lower atmosphere and upper thermosphere during the SSW event. More importantly, the global observations of COSMIC EDPs, as well as peak density (NmF2) and peak height (hmF2) in the F2 region from the EDPs, provide a unique opportunity to gain important insight of dynamic processes that might contribute to the ionosphere-thermosphere variability during the SSW.

2. COSMIC Data and the January 2009 SSW Event

[5] COSMIC consists of six identical microsatellites launched on April 2006. The primary instruments are GPS RO receivers. Each spacecraft utilizes four GPS antennas: two occultation antennas for 50 Hz tracking for atmospheric profiling in an open-loop (OL) mode and two single patch antennas for 1 Hz tracking for precise orbit determination (POD) and ionospheric profiling [*Rocken et al.*, 2000; *Schreiner et al.*, 2007]. These payloads are managed by the University Corporation for Atmospheric Research (UCAR), and the raw observations are processed by the COSMIC Data Analysis and Archive Center (CDAAC) both in near real time and postprocessing. The GPS RO amplitude and phase observations are used to compute the bending angle of GPS ray that is then inverted into profiles of refractivity and such meteorological parameters as pressure, temperature, and humidity under certain assumptions or via direct assimilation by atmospheric models [*Kuo et al.*, 2004; *Schreiner et al.*, 2007; *Sokolovskiy et al.*, 2006]. Phase observations from the POD antenna are used to obtain EDPs [*Lei et al.*, 2007; *Schreiner et al.*, 1999]. Both the neutral atmospheric and the ionospheric inversions use the assumption of local spherical symmetry of refractivity (Abel inversion) and assign the retrieved parameters to the ray tangent points. The Abel retrievals can have significant systematic errors below the F layer in regions with large horizontal gradients but give reasonable EDPs in the F and above region as well as NmF2 and hmF2 [e.g., *Lei et al.*, 2007; *Yue et al.*, 2010]. Note that the systematic errors of the Abel retrievals as demonstrated by *Yue et al.* [2010] do not significantly affect this study because it focuses on the relative changes in electron density between the non-SSW and SSW days.

[6] This work uses the COSMIC retrieved neutral temperature profiles between 10 and 60 km around January 2009 to illustrate the evolution of the 2009 SSW event. The National Center for Atmospheric Research (NCAR) National Centers for Environmental Prediction (NCEP) zonal mean zonal wind is also used here [*Kalnay et al.*, 1996], given that the temperature observations alone cannot determine whether it is a major or minor SSW event. As shown in Figure 1, a major SSW event occurred during late January and early February of 2009. The warming mainly occurred below 40 km and started at about 20 January. The temperature around 35 km increased by as much as 50 K during these days. The peak of this SSW propagates downward with time. It took about 20 days for the temperature to recover between 20 and 40 km. Below 20 km, there was a steady warming since 27 January with several Kelvin amplitude, lasting more than 2 months. Concurrently with the stratospheric warming, there was a cooling above 45 km with the largest amplitude more than 60 K. This is in accordance with *Liu and Roble* [2002] simulation work and also the independent observations of 2009 SSW by *Manney et al.* [2009]. Note that the COSMIC retrieved temperatures

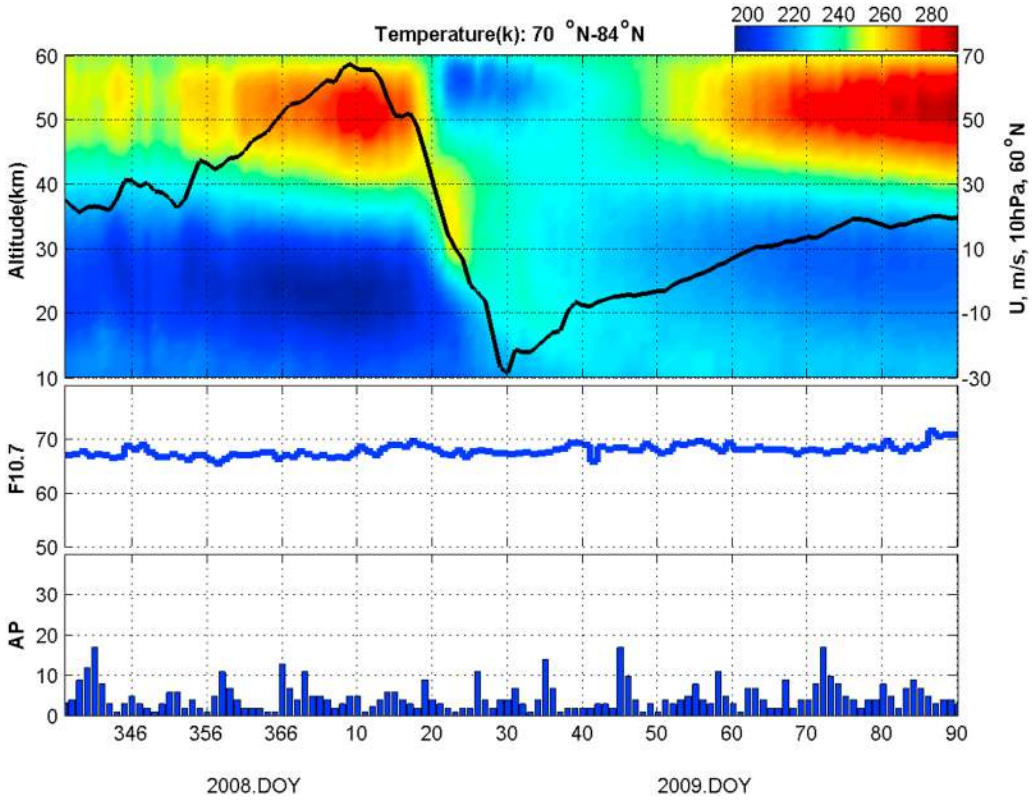

Figure 1. Variations of zonal mean neutral temperature averaged between 70°N and 84°N in (top) the altitude range of 10 and 60 km from COSMIC (contour) and NCEP zonal mean zonal wind (black curve) at 10 hPa altitude and 60°N, (middle) F10.7, and (bottom) Ap index as a function of day number in 2009.

at those heights might be more influenced by the background model used in the data retrieval [*Ho et al.*, 2009]. The NCEP zonal mean zonal wind at 10 hPa (~30 km) of 60°N decreased during the whole SSW event, while it reversed around 25 January and reached strongest westward wind (~30 m/s) at about 30 January. Detailed information about the temperature and circulation of 2009 SSW event from COSMIC and NCEP data can be found in the work of *Taylor and Randel* [2009]. In addition, solar activity index F10.7 and geomagnetic activity AP index, shown in Figure 1, indicate that the solar and geomagnetic activities were low during and around the 2009 SSW event. As mentioned before, it is an ideal period to study the variability of ionosphere resulting from the lower atmosphere when the day-to-day changes of solar irradiation and magnetospheric energy are minimized.

[7] According to *Goncharenko et al.* [2010a, 2010b], the low-latitude TEC and ionospheric electric field responses during 2009 SSW event peak during 26–30 January. There was a minor storm during 26 January as indicated from the AP index in Figure 1. To avoid the possible contamination of this minor storm effect in our results, 27–30 January was chosen as SSW period. Although the 2009 SSW lasts for more than 20 days as indicated from Figure 1, only the days when ionospheric density as well as electric field has maximum response were chosen as SSW days here. At the same time, 14–18 January was chosen as a reference (non-SSW) period. We chose the 5 days prior to the start of the SSW event as reference quiet days to minimize the effects of ionospheric and nonmigrating tides seasonal variation on our analysis results. As indicated by *Vineeth et al.* [2009], the planetary wave amplitude might be enhanced during the period of ~1 month before the SSW in the equatorial mesopause region. However, no preconditioning effect was detected in the ionosphere response during 2009 SSW in the previous studies [*Fejer et al.*, 2010; *Goncharenko et al.*, 2010a, 2010b]. Thus, our choice for the reference should be reasonable. The COSMIC observed EDPs are then binned into geomagnetic latitude, longitude, and local time cells with the intervals of 5°, 10°, and 1 h, respectively, for both non-SSW and SSW days. If there are observed EDPs during both non-SSW days and SSW days for the same cell, then it is considered as a case. If more than one EDP is available in the same cell for non-SSW days or SSW days, an average EDP is used. The day-to-day variability of COSMIC NmF2 and hmF2 is generally estimated by binning the data during 40 days observed before this SSW event in the same geo-location and local time cell, and it is found that the average root mean square error is ~5% for NmF2 and ~2 km for hmF2. According to the results of *Goncharenko and Zhang* [2008], *Goncharenko et al.* [2010a, 2010b], and *Chau et al.* [2009], the ionospheric response including ion temperature, electron density, and vertical drift during SSW event mainly occurs in the daytime. This study only concentrates on the observations during the daytime. *Goncharenko et al.* [2010a, 2010b] shows that the ionospheric TEC response in low latitude mainly increases in the morning and decreases in the afternoon with the switch time

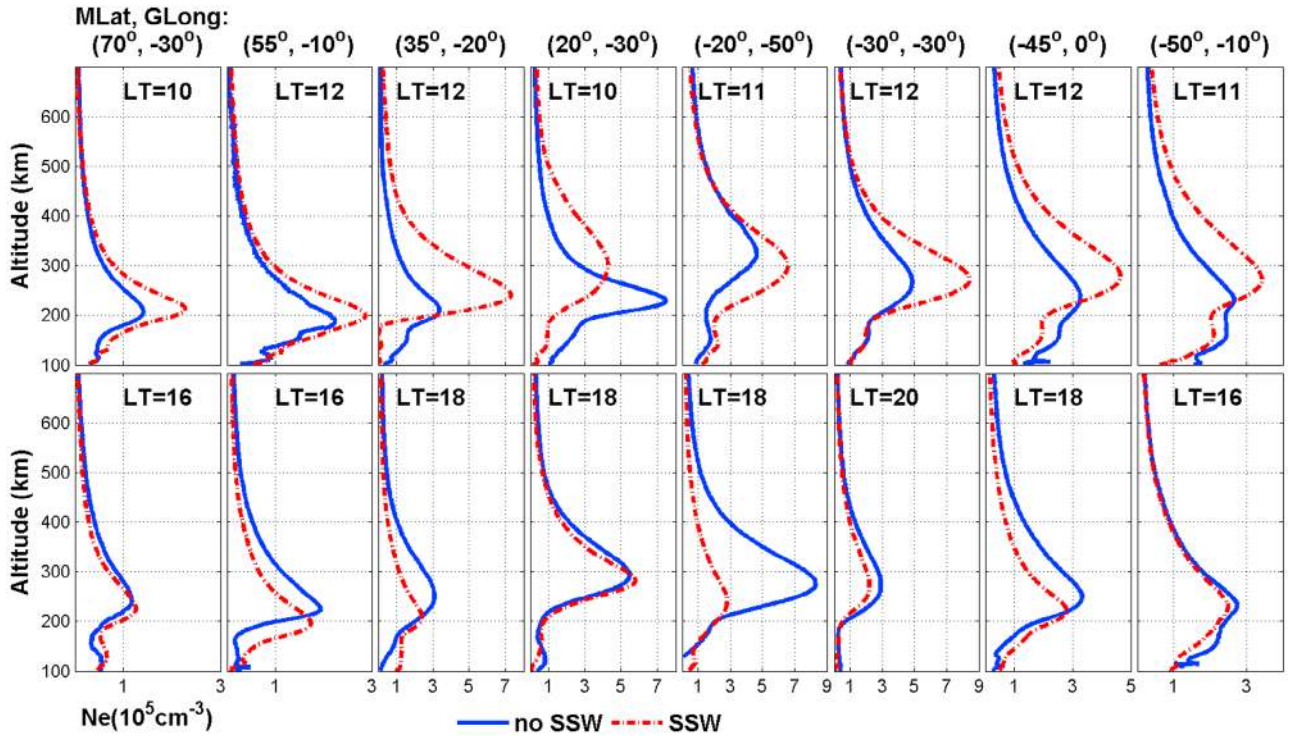

Figure 2. Electron density profiles during SSW (dashed lines) and non-SSW days (solid lines) in both (top) morning and (bottom) afternoon sectors around the same location and local time bins over American and Atlantic sectors. The corresponding geomagnetic latitude and geographic longitude and the local time are shown.

shift with the increase of day number. Local times range of 8–13 and 16–20 h, when the low-latitude ionospheric TEC increases and decreases during the selected SSW days, were chosen to represent the morning and afternoon sectors, respectively. There are totally 671 cases, including 352 cases in the morning and 319 in the afternoon. In section 3, the global measurements of EDPs from COSMIC are utilized to analyze the ionospheric response during the January 2009 SSW event.

3. Ionospheric Response During SSW

[8] Figure 2 shows eight EDPs over the American and Atlantic sectors (60°W–0°) as an example. In addition to the selection criterion described above, each profile in both morning and afternoon sectors was observed in the same location cell. In the morning, electron density for all the cases increases significantly during the SSW days in comparison with that of non-SSW days except the case over (20° geomagnetic latitude, −30° longitude). At the same time, the increase of the peak height of the F2 region can be seen clearly. The prominent increase appears in low latitude, where the background electron density is relatively large. The relative increase of NmF2 can reach as high as 150%. In the low latitude region, the increase of hmF2 can exceed 100 km. In the afternoon, all the selected cases show obvious decrease in electron density as well as peak height. NmF2 over (−20°, −50°) is larger by 100% in the afternoon than that of morning during non-SSW days, while NmF2 in the afternoon decreases to 50% of the morning sector value during SSW days. The severe disturbance occurs over (35°, −20°), where NmF2 increases by 150% in the morning and decreases by 40% in the afternoon.

[9] Next a statistical analysis was performed for the peak electron density (NmF2), peak height (hmF2), and ionospheric TEC (ITEC; integration between 100 and 700 km for each electron density profile). The relative deviation of NmF2 and ITEC and absolute deviation of hmF2 during the SSW days from that of non-SSW days for the selected 671 cases are computed. Figure 3 depicts the statistical results. Generally, all three parameters increase in the morning and decrease mostly in the afternoon globally, which compares well with the case studies in Figure 2. The details of the statistical results are given in Table 1, in which the statistical numbers of increase and decrease with absolute value of relative deviation of NmF2 and ITEC larger than 10% and absolute deviation of hmF2 greater than 10 km. The changes of NmF2 and ITEC less than 10% or absolute deviation of hmF2 lower than 10 km are considered to be associated with the day-to-day variability of the ionosphere and observational error. The estimated variability of NmF2 and hmF2 before 2009 SSW is ~5% and 2 km, respectively. As indicated by *Yue et al.* [2010], the standard deviation of Abel retrieved error of NmF2 (relative) and hmF2 (absolute) are ~15% and ~7 km, respectively. Usually the root mean square error is smaller than the standard deviation. So it is reasonable for us to choose the threshold of 10% for NmF2 and ITEC and 10 km for hmF2 to do the statistical analysis here. There are a total of 262 cases satisfying this criterion in all the 671 selected cases, and 112 of them occur in the morning and 150 in the afternoon. Obviously, all three parameters increase mainly in the morning and decrease in the afternoon in the

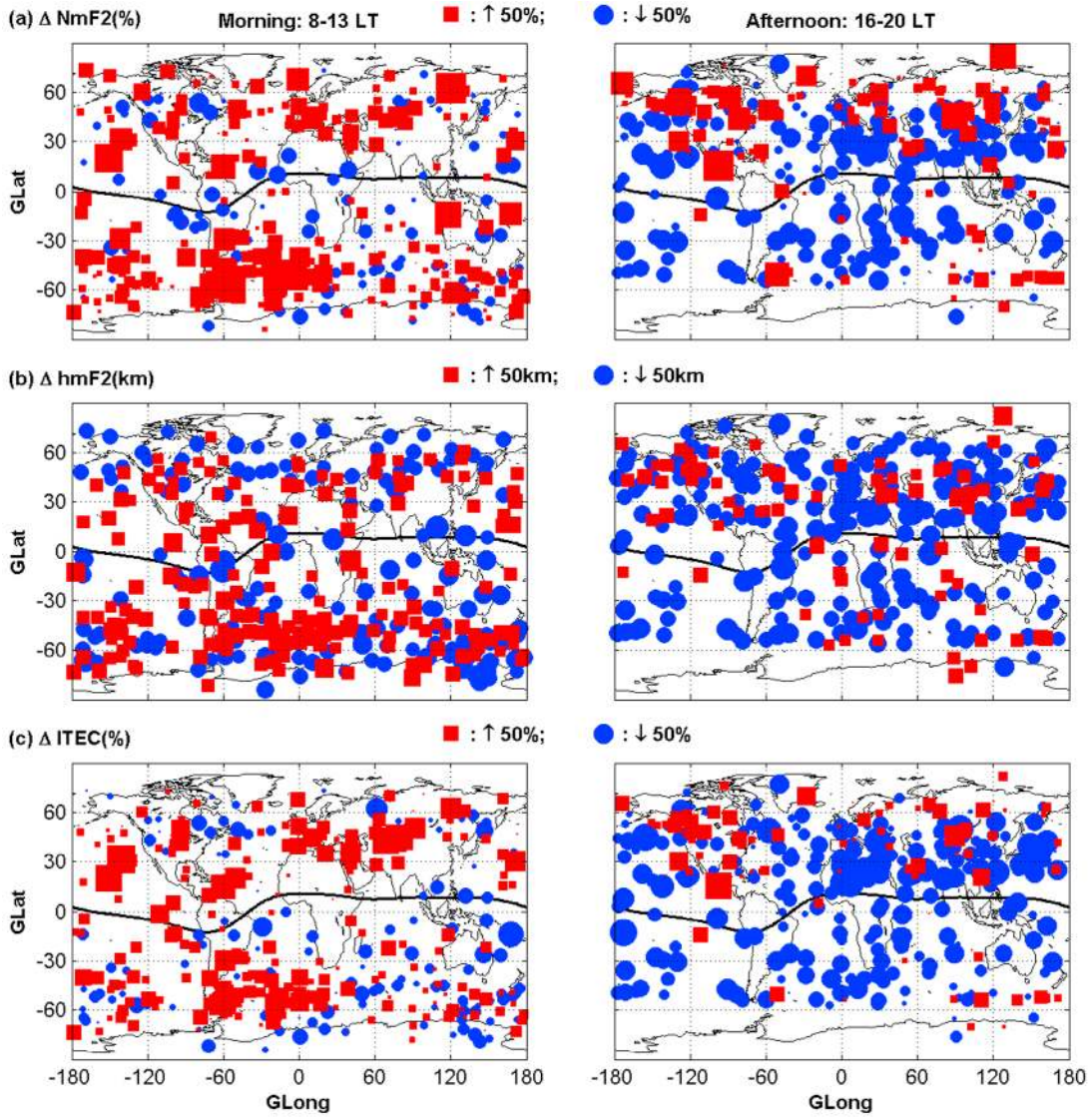

Figure 3. Global distributions of increase (squares) and decrease (circles) cases for (a) NmF2 (in %), (b) hmF2 (in km), and (c) ITEC (in %) during (left) morning (8–13 LT) and (right) afternoon (16–20 LT) sectors for the SSW days relative to non-SSW days. The size of the squares and circles represent the amplitudes of increase and decrease, respectively. The black line shows the Dip equator.

middle and low latitude region (MLat < 60°). In the high latitude (MLat ≥ 60°), all three parameters show increase in the afternoon, which is different from that of middle- and low-latitude region; the increase in the morning is not significant and hmF2 even shows decrease in the morning. Quantitatively, the probability of cases that show increases in NmF2, hmF2, and ITEC in the morning sector is 73%, 65%, and 76%, respectively, while the case showing decreases in the afternoon is 77%, 77%, and 81%. The average value of relative deviation of NmF2 and ITEC and absolute deviation of hmF2 is shown in Table 2. The NmF2, hmF2, and ITEC on average increase 19%, 12 km, and 17% in the morning and decrease 23%, 19 km, and 25% in the afternoon, respectively, during the SSW in comparison with the corresponding values during non-SSW days. Additionally, the high-latitude region shows increased NmF2 and ITEC and decreased hmF2 during either morning or afternoon, which is different from that of middle and low latitude region. No longitude variation can be found in the figure. The middle- and high-latitude of Northern Hemisphere has relatively more increase cases in the afternoon than Southern Hemisphere.

[10] As shown in the Figures 2 and 3, both the ionospheric electron densities and peak height increase in the morning and decrease in the afternoon mostly during this SSW event, especially in middle- and low-latitude region. This result agrees with that of *Goncharenko et al.* [2010a, 2010b]. However, *Goncharenko et al.* [2010a, 2010b] mainly concentrated on the TEC observations in the low-middle latitudes. According to *Goncharenko et al.* [2010a, 2010b] and *Fejer et al.* [2010], the vertical drift over Jicamarca increases in the morning and decreases in the afternoon during the SSW days in comparison with the days before the SSW, which can be used to explain the disturbance of the ionosphere in the low-latitude and equatorial regions. It is

Table 1. Statistical Case Numbers for Increased and Decreased NmF2, hmF2, and ITEC[a]

	MLat ≤ 30°		30° < MLat < 60°		MLat ≥ 60°		Total	
	Morning	Afternoon	Morning	Afternoon	Morning	Afternoon	Morning	Afternoon
				Number of Sample				
	39	80	51	56	22	14	112	150
				Increase Number (%)				
NmF2	24 (62%)	8 (10%)	43 (84%)	15 (27%)	15 (68%)	11 (79%)	82 (73%)	34 (23%)
hmF2	25 (64%)	15 (19%)	39 (76%)	9 (16%)	9 (41%)	10 (71%)	73 (65%)	34 (23%)
ITEC	32 (82%)	6 (8%)	40 (78%)	13 (23%)	13 (59%)	10 (71%)	85 (76%)	29 (19%)
				Decrease Number (%)				
NmF2	15 (38%)	72 (90%)	8 (16%)	41 (73%)	7 (32%)	3 (21%)	30 (27%)	116 (77%)
hmF2	14 (36%)	65 (81%)	12 (24%)	47 (84%)	13 (59%)	4 (29%)	39 (35%)	116 (77%)
ITEC	7 (18%)	74 (92%)	11 (22%)	43 (77%)	9 (41%)	4 (29%)	27 (24%)	121 (81%)

[a]During SSW days in comparison with those during non-SSW days and the corresponding percentage in the total sample number over equatorial and low-latitude area (MLat ≤ 30°), middle-latitude area (30° < MLat < 60°), high-latitude area (MLat ≥ 60°), and all latitudes together (total) during the morning (8–13 LT) and afternoon (16–20 LT) sectors. Only cases with changes of ΔNmF2 and ΔITEC larger than 10% and ΔhmF2 higher than 10 km are considered here.

generally thought that these vertical drift disturbances during SSW are the result of interactions between planetary waves and tidal modes through *E* region dynamo processes [*Goncharenko et al.*, 2010a, 2010b; *Liu et al.*, 2010]. *Vineeth et al.* [2009] found that the planetary wave around the dynamo region (mesopause region) indeed enhanced during SSW period by comparing the observed equatorial mesopause temperature during SSW period with that of non-SSW period. The tides which interact with the planetary wave can be either semidiurnal lunar tide or diurnal and semidiurnal migrating and nonmigrating tides [*Fejer et al.*, 2010; *Liu et al.*, 2010]. In addition, the effect of disturbance on neutral background resulted from the direct propagation of tides from the lower atmosphere cannot be ruled out. The results of this study show that electron densities also present significant changes in the high-middle latitude regions, which cannot be explained by the low-middle *E* region dynamo mechanism. Alternatively, the upper thermospheric properties, particularly neutral winds, can be modulated significantly due to planetary wave and tide interactions [*Liu et al.*, 2010], and they might contribute to the observed ionospheric variations at high-middle latitudes from the COSMIC measurements. Further investigation is required of this mechanism.

[11] As mentioned previously, the changed vertical drift is considered to be the main reason of low-latitude and equatorial ionospheric response during the SSW event [*Chau et al.*, 2009; *Goncharenko et al.*, 2010a, 2010b]. If this is the case, the increased (decreased) upward vertical drift will result in the enhancement (weakening) of NmF2 at middle and low latitudes because of the fountain effect, while it lead to a opposite response in the equatorial region . For hmF2, it will increase over the whole middle-low latitude and equatorial region because of the uplifting effect of vertical drift and vice versa. From Figures 2 and 3, an increase (decrease) is seen in hmF2 and a decrease (increase) in NmF2 in the morning (afternoon) for some cases over equatorial region, which generally support the electric field mechanism, as suggested by *Goncharenko et al.* [2010a, 2010b]. However, there are some exceptional cases, in which electron densities increase in the morning and decrease in the afternoon. It is known that the ionosphere in the F2 region is controlled not only by the electric field but also by the neutral thermosphere such as neutral composition and neutral wind, while the latter also can be modulated by tides. These exceptional cases support our assumption of direct penetration of tides from the lower atmosphere into the ionosphere F2 region given in the above. In the middle and high latitudes, the cases with decrease of NmF2 and hmF2 in the morning and increase in the afternoon with relatively larger amplitude may be suggestive of the competitive effects of electric field and background neutral gas. Furthermore, the modified regional polarized electric field due to the wave propagation and the interaction between the planetary wave and tides [see *Liu et al.*, 2010] might also play an important role in producing the complex ionospheric response during the SSW in different regions. Finally, it should be pointed out that our study provides an interesting database for future modeling efforts, which are certainly necessary to understand the physical processes of the coupling between the ionosphere and the lower atmosphere that might contribute to the ionosphere-thermosphere variability during the SSW.

[12] According to *Fejer et al.* [2010], the onset of equatorial afternoon counter electrojet during SSW event has a longitudinal dependency [*Liu et al.*, 2010]. It implies that

Table 2. Average Value of Relative Deviation of NmF2 and ITEC and Absolute Deviation of hmF2[a]

	Mlat ≤ 30°		30° < MLat < 60°		MLat ≥ 60°		Total	
	Morning	Afternoon	Morning	Afternoon	Morning	Afternoon	Morning	Afternoon
ΔNmF2(%)	12	−34	26	−18	16	24	19	−23
ΔhmF2(km)	18	−26	18	−20	−15	−16	12	−19
ΔITEC(%)	17	−36	19	−22	11	13	17	−25

[a]Over equatorial and low-latitude area (MLat ≤ 30°), middle-latitude area (30° < MLat < 60°), high-latitude area (MLat ≥ 60°), and all latitudes together (Total) during the morning (8–13 LT) and afternoon (16–20 LT) sectors.

the ionosphere response might have longitudinal variation at least in low-latitude area. However, no longitude variations were detected from the COSMIC data. Note that we put the data on SSW days together and divided them into the morning and afternoon bins. This might eliminate the longitude variation if it indeed has day-to-day variability or local time dependence [*Fejer et al.*, 2010; *Liu et al.*, 2010]. We also found that the increase of all three parameters is stronger in the Northern Hemisphere than in the Southern Hemisphere during the afternoon time. The occurrence of SSW in the northern polar region makes the Northern Hemisphere more disturbed through tides upward propagation and influences the dynamo region by planetary-tides interaction. This might contribute to this hemisphere asymmetry. Some researches also show that the ionosphere response during SSW has a local time shift with the increase of the day number [*Fejer et al.*, 2010; *Goncharenko et al.*, 2010a, 2010b]. During 2009 SSW event, the increase of low-latitude TEC occurs during 7–13 LT on 26 January, while it is ~9–15 LT on 30 January [*Goncharenko et al.*, 2010b]. However, only 671 cases were found from COSMIC data in this study, so that the local time shift effect cannot be properly determined.

4. Conclusion

[13] A major SSW event occurred during January 2009, when the solar activity was extremely low. It provides a good opportunity to study the variability of the ionosphere resulting from lower atmospheric phenomena. This investigation studied the global ionospheric response during the January 2009 SSW event for the first time by using integrated observations of the neutral atmosphere and ionosphere from the COSMIC satellites. Six hundred seventy-one cases that have EDP observations during both SSW days and the selected reference non-SSW days in the same latitude-longitude-local time cell were chosen to conduct the statistical analysis. It was found that the ionospheric peak density, peak height, and TEC increase in the morning hours and decrease in the afternoon globally in ~75% of the cases during the SSW days in comparison with no SSW days. NmF2, hmF2, and ITEC, on average, increase 19%, 12 km, and 17% in the morning and decrease 23%, 19 km, and 25% in the afternoon, respectively, from global COSMIC observations. These results are in good agreement with previous results from TEC observations [*Goncharenko et al.*, 2010a, 2010b] in the low-latitude and equatorial regions.

[14] Interestingly, the unique COSMIC observations also revealed that during this SSW the ionosphere responds globally not only in low-latitude and equatorial regions but also at high and middle latitudes. In the high-latitude region, the ionosphere displayed increase of NmF2 and ITEC and decrease of hmF2 during either morning or afternoon sector during SSW days, which is different from that of the middle and low latitude region. The ionospheric response in the low-middle latitude and equatorial regions during this SSW event can be explained by either the disturbed vertical drift resulting from the interaction between the planetary waves and tides through *E* region dynamo or the direct penetration of tides, whereas the ionospheric variations at middle and high latitudes during SSW might also be attributed to the neutral wind and composition disturbance resulting from direct propagation of tides from the lower atmosphere to the ionospheric F2 region. However, the existence of competitive effects of different controlling factors such as the electric field, neutral wind, and composition might result in the observed complicated global ionospheric changes during the January 2009 SSW event.

[15] **Acknowledgments.** This work is supported by National Science Foundation under grant AGS-0961147. We acknowledge the whole CDAAC team for processing the COSMIC data and making the data available. NCEP Reanalysis Derived data are provided by the NOAA/OAR/ESRL PSD, Boulder, Colorado, USA (http://www.esrl.noaa.gov/psd/). The F107 and Ap indices are downloaded from the SPIDR Web site http://spidr.ngdc.noaa.gov/.

[16] Robert Lysak thanks the reviewers for their assistance in evaluating this paper.

References

Abdu, M. A., T. K. Ramkumar, I. S. Batista, C. G. M. Brum, H. Takahashi, B. W. Reinisch, and J. H. A. Sobral (2006), Planetary wave signatures in the equatorial atmosphere-ionosphere system, and mesosphere-*E* and *F* region coupling, *J. Atmos. Sol. Terr. Phys.*, *68*, 509–522.

Charlton, A. J., and L. M. Polvani (2007), A new look at stratospheric sudden warmings: Part I. Climatology and modeling benchmarks, *J. Clim.*, *20*, 449–469.

Chau, J. L., B. G. Fejer, and L. P. Goncharenko (2009), Quiet variability of equatorial E × B drifts during a sudden stratospheric warming event, *Geophys. Res. Lett.*, *36*, L05101, doi:10.1029/2008GL036785.

Fejer, B. G., M. E. Olson, J. L. Chau, C. Stolle, H. Lühr, L. P. Goncharenko, K. Yumoto, and T. Nagatsuma (2010), Lunar dependent equatorial ionospheric electrodynamics effects during sudden stratospheric warmings, *J. Geophys. Res.*, *115*, A00G03, doi:10.1029/2010JA015273.

Forbes, J. M., and S. Leveroni (1992), Quasi 16-day oscillation in the ionosphere, *Geophys. Res. Lett.*, *19*(10), 981–984, doi:10.1029/92GL00399.

Fuller-Rowell, T. J., et al. (2008), Impact of terrestrial weather on the upper atmosphere, *Geophys. Res. Lett.*, *35*, L09808, doi:10.1029/2007GL032911.

Goncharenko, L., and S.-R. Zhang (2008), Ionospheric signatures of sudden stratospheric warming: Ion temperature at middle latitude, *Geophys. Res. Lett.*, *35*, L21103, doi:10.1029/2008GL035684.

Goncharenko, L. P., J. Chau, H.-L. Liu, and A. J. Coster (2010a), Unexpected connections between the stratosphere and ionosphere, *Geophys. Res. Lett.*, *37*, L10101, doi:10.1029/2010GL043125.

Goncharenko, L. P., A. J. Coster, J. L. Chau, and C. E. Valladares (2010b), Impact of sudden stratospheric warmings on equatorial ionization anomaly, *J. Geophys. Res.*, *115*, A00G07, doi:10.1029/2010JA015400.

Ho, S.-P., et al. (2009), Estimating the uncertainty of using GPS radio occultation data for climate monitoring: Intercomparison of CHAMP refractivity climate records from 2002 to 2006 from different data centers, *J. Geophys. Res.*, *114*, D23107, doi:10.1029/2009JD011969.

Kalnay, E., et al. (1996), The NCEP/NCAR 40 year reanalysis project, *Bull. Am. Meteorol. Soc.*, *77*, 437–470.

Kuo, Y.-H., T.-K. Wee, S. Sokolovskiy, C. Rocken, W. Schreiner, D. Hunt, and R. A. Anthes (2004), Inversion and error estimation of GPS radio occultation data, *J. Meteorol. Soc. Jpn.*, *82*, 507–531.

Lăstovička, J., and B. A. de la Morena (1987), The response of the lower ionosphere in central and southern Europe to anomalous stratospheric conditions, *Phys. Scripta.*, *35*, 902–905.

Lăstovička, J., P. Križan, P. Šauli, and D. Novotná (2003), Persistence of the planetary wave type oscillations in foF2 over Europe, *Ann. Geophys.*, *21*, 1543–1552.

Lei, J., et al. (2007), Comparison of COSMIC ionospheric measurements with ground-based observations and model predictions: Preliminary results, *J. Geophys. Res.*, *112*, A07308, doi:10.1029/2006JA012240.

Liu, H.-L., and R. G. Roble (2002), A study of a self-generated stratospheric sudden warming and its mesospheric-lower thermospheric impacts using the coupled TIME-GCM/CCM3, *J. Geophys. Res.*, *107*(D23), 4695, doi:10.1029/2001JD001533.

Liu, H.-L., W. Wang, A. D. Richmond, and R. G. Roble (2010), Ionospheric variability due to planetary waves and tides for solar minimum conditions, *J. Geophys. Res.*, *115*, A00G01, doi:10.1029/2009JA015188.

Manney, G. L., M. J. Schwartz, K. Krüger, M. L. Santee, S. Pawson, J. N. Lee, W. H. Daffer, R. A. Fuller, and N. J. Livesey (2009), Aura Microwave Limb Sounder observations of dynamics and transport during the

record-breaking 2009 Arctic stratospheric major warming, *Geophys. Res. Lett.*, *36*, L12815, doi:10.1029/2009GL038586.

Rishbeth, H. (2006), *F* region links with the lower atmosphere?, *J. Atmos. Sol. Terr. Phys.*, *68*, 469–478.

Rishbeth, H., and M. Mendillo (2001), Patterns of ionospheric variability, *J. Atmos. Sol. Terr. Phys.*, *63*, 1661–1680.

Rocken, C., Y.-H. Kuo, W. Schreiner, D. Hunt, S. Sokolovskiy, and C. McCormick (2000), COSMIC system description, *Terr. Atmos. Oceanic Sci.*, *11*(1), 21–52.

Schreiner, W. S., S. V. Sokolovskiy, C. Rocken, and D. C. Hunt (1999), Analysis and validation of GPS/MET radio occultation data in the ionosphere, *Radio Sci.*, *34*(4), 949–966.

Schreiner, W., C. Rocken, S. Sokolovskiy, S. Syndergaard, and D. Hunt (2007), Estimates of the precision of GPS radio occultations from the COSMIC/FORMOSAT-3 mission, *Geophys. Res. Lett.*, *34*, L04808, doi:10.1029/2006GL027557.

Sokolovskiy, S., C. Rocken, D. Hunt, W. Schreiner, J. Johnson, D. Masters, and S. Esterhuizen (2006), GPS profiling of the lower troposphere from space: Inversion and demodulation of the open-loop radio occultation signals, *Geophys. Res. Lett.*, *33*, L14816, doi:10.1029/2006GL026112.

Sridharan, S., S. Sathishkumar, and S. Gurubaran (2009), Variabilities of mesospheric tides and equatorial electrojet strength during major stratospheric warming events, *Ann. Geophys.*, *27*, 4125–4130.

Taylor, J. R., and W. J. Randel (2009), COSMIC observations of the stratospheric sudden warming of January 2009, in *The 4th COSMIC Data User Workshop*, Natl. Cent. for Atmos. Res., Boulder, Colo.

Vineeth, C., T. K. Pant, C. V. Devasia, and R. Sridharan (2007), Atmosphere-Ionosphere coupling observed over the dip equatorial MLTI region through the quasi 16 day wave, *Geophys. Res. Lett.*, *34*, L12102, doi:10.1029/2007GL030010.

Vineeth, C., T. K. Pant, K. K. Kumar, G. Ramkumar, and R. Sridharan (2009), Signatures of low latitude–high latitude coupling in the tropical MLT region during sudden stratospheric warming, *Geophys. Res. Lett.*, *36*, L20104, doi:10.1029/2009GL040375.

Wan, W., H. Yuan, B. Ning, J. Liang, and F. Ding (1998), Traveling ionospheric disturbances associated with the tropospheric vortexes around Qinghai-Tibet Plateau, *Geophys. Res. Lett.*, *25*(20), 3775–3778, doi:10.1029/1998GL900030.

Xiong, J., W. Wan, B. Ning, L. Liu, and Y. Gao (2006), Planetary wave-type oscillations in the ionosphere and their relationship to mesospheric/lower thermospheric and geomagnetic disturbances at Wuhan (30.61°N, 114.51°E), *J. Atmos. Sol. Terr. Phys.*, *68*, 498–508.

Yue, X., W. S. Schreiner, J. Lei, S. V. Sokolovskiy, C. Rocken, D. C. Hunt, and Y.-H. Kuo (2010), Error analysis of Abel retrieved electron density profiles from radio-occultation measurements, *Ann. Geophys.*, *28*, 217–222.

Zhao, B., W. Wan, L. Liu, K. Igarashi, M. Nakamura, L. J. Paxton, S.-Y. Su, G. Li, and Z. Ren (2008), Anomalous enhancement of ionospheric electron content in the Asian-Australian region during a geomagnetically quiet day, *J. Geophys. Res.*, *113*, A11302, doi:10.1029/2007JA012987.

D. C. Hunt, Y.-H. Kuo, C. Rocken, W. S. Schreiner, and X. Yue, COSMIC Program Office, University Corporation for Atmospheric Research, Boulder, CO 80307, USA. (xinanyue@ucar.edu)

J. Lei, Department of Aerospace Engineering Sciences, University of Colorado, Boulder, CO 80309, USA.

W. Wan, Institute of Geology and Geophysics, Chinese Academy of Sciences, Beijing 100029, China.